



OPEN ACCESS

EDITED BY

Qing Pan,
Qingdao Agricultural University, China

REVIEWED BY

Xin Cao,
Jilin Agricultural University, China
Fusheng Si,
Shanghai Academy of Agricultural
Sciences, China

*CORRESPONDENCE

Shuangbao Gun
✉ gunsbao056@126.com

SPECIALTY SECTION

This article was submitted to
Infectious Agents and Disease,
a section of the journal
Frontiers in Microbiology

RECEIVED 11 November 2022

ACCEPTED 28 December 2022

PUBLISHED 12 January 2023

CITATION

Yang J, Zhang J, Yang Q, Huang X,
Yan Z, Wang P, Gao X, Li J, Li N, Gao Y
and Gun S (2023) LncRNA *EN-90756*
promotes CPB2-induced proliferation
and inhibits apoptosis in IPEC-J2 cells
by affecting the JAK-STAT signaling
pathway activation.
Front. Microbiol. 13:1082025.
doi: 10.3389/fmicb.2022.1082025

COPYRIGHT

© 2023 Yang, Zhang, Yang, Huang,
Yan, Wang, Gao, Li, Li, Gao and Gun.
This is an open-access article
distributed under the terms of the
[Creative Commons Attribution License
\(CC BY\)](https://creativecommons.org/licenses/by/4.0/). The use, distribution or
reproduction in other forums is
permitted, provided the original
author(s) and the copyright owner(s)
are credited and that the original
publication in this journal is cited, in
accordance with accepted academic
practice. No use, distribution or
reproduction is permitted which does
not comply with these terms.

LncRNA *EN-90756* promotes CPB2-induced proliferation and inhibits apoptosis in IPEC-J2 cells by affecting the JAK-STAT signaling pathway activation

Jiaojiao Yang¹, Juanli Zhang², Qiaoli Yang¹, Xiaoyu Huang¹,
Zunqiang Yan¹, Pengfei Wang¹, Xiaoli Gao¹, Jie Li¹, Na Li³,
Yi Gao³ and Shuangbao Gun^{1,4*}

¹College of Animal Science and Technology, Gansu Agricultural University, Lanzhou, China,

²College of Life Sciences and Technology, Longdong University, Qingyang, China, ³Jilin Rongtai Agricultural Development Co., Ltd., Changchun, China, ⁴Gansu Research Center for Swine Production Engineering and Technology, Lanzhou, China

Background: Long non-coding RNAs (lncRNAs), as key regulators, are closely associated with the development of a variety of disease. However, the mechanisms by which lncRNAs regulate *Clostridium perfringens* type C induced piglet diarrhea are unclear.

Methods: In the present study, we explored the expression and characterization of lncRNAs in a *C. perfringens* beta2 (CPB2) toxin-treated intestinal porcine epithelial cell line-J2 (IPEC-J2) using RNA-sequencing (RNA-seq).

Results: A total of 6,558 lncRNAs were identified, of which 49 lncRNAs were significantly differentially expressed between the control and CPB2 groups. Functional enrichment analysis showed that the target genes of differentially expressed lncRNA *EN-90756* were mainly associated with defense response to virus, and negative regulation of apoptotic process. LncRNA *EN-90756* was significantly up-regulated in IPEC-J2 cells at different time points after CPB2 treatment. Functionally, knockdown of lncRNA *EN-90756* might regulate the proliferation and apoptosis of IPEC-J2 cells by affecting the Janus kinase (JAK)-signal transducer and activator of transcription (STAT) signaling pathway. LncRNA *EN-90756* may be involved in CPB2 toxin-induced piglet diarrhea by regulating the expression of its target gene *MX1* (encoding MX dynamin like GTPase 1).

Conclusion: Long non-coding RNA *EN-90756* affected the antiviral ability of IPEC-J2 cells by regulating the expression of *MX1*. Meanwhile, lncRNA

EN-90756 might regulate cell proliferation and apoptosis by affecting JAK-STAT signaling pathway activation. These findings provide novel perspectives and directions for further exploration of the regulatory mechanisms of lncRNAs on CPB2 toxin-induced diarrhea in piglets.

KEYWORDS

RNA-seq, lncRNAs, IPEC-J2, CPB2 toxin, piglet diarrhea

1. Introduction

Piglet diarrhea has a high incidence and brings huge economic losses to pig farms (Silva et al., 2015). *Clostridium perfringens* type C is one of the main pathogens causing diarrhea in piglets, producing *C. perfringens* beta2 (CPB2) toxin that acts directly or indirectly on the intestines, causing intestinal damage and triggering an inflammatory response (Zeng et al., 2016). Several epidemiological studies suggested that CPB2 toxins are highly associated with intestinal diseases in domestic animals. NetB toxin and CPB2 toxin produced by *C. perfringens* are associated with subclinical necrotizing enteritis in laying hens (Timoney et al., 2005). CPB2 toxin might play a role in the pathogenesis of enterotoxaemia in calves (Lebrun et al., 2007). There is a significant association between CPB2-positive *C. perfringens* isolates and piglet diarrhea (Waters et al., 2003). CPB2 toxin is significantly cytotoxic to intestinal porcine epithelial cell line-J2 (IPEC-J2) cells inhibiting cell growth and increasing cell permeability in a concentration-dependent manner (Luo et al., 2020). CPB2 toxin induces apoptosis and increases inflammatory markers in IPEC-J2 cells and impairs intestinal barrier function (Gao et al., 2020).

Long non-coding RNAs (lncRNAs) are RNAs comprising more than 200 nucleotides that have almost no protein-coding capacity and play key roles in a variety of biological processes, including epigenetic regulation, transcriptional regulation, metabolism, and immune responses (Marzia et al., 2018). In recent years, studies have reported that lncRNAs have important functions in piglet resistance to pathogenic infections causing diarrhea. Down-regulation of lncRNA *FUT3-AS1* expression contributed to enhancing the resistance of IPEC-J2 cells to *Escherichia coli* F18 infection (Wu et al., 2022). Porcine endemic diarrhea virus (PEDV) infection modulates lncRNA expression patterns in the ileum of IPEC-J2 cell lines and piglets and activates the ileal immune system (Chen et al., 2019). In piglet diarrhea caused by *C. perfringens* type C, many lncRNAs and mRNAs modulate drug resistance and susceptibility in piglets through immune-related pathways (Huang et al., 2019). Although many lncRNAs have been reported to be associated with piglet diarrhea, few lncRNAs have been identified that are closely associated with CPB2 toxin-induced diarrhea in piglets.

Our previous study used CPB2 toxin (20 µg/ml) to treat IPEC-J2 cells for 24 h to construct an *in vitro* model of *C. perfringens* type C infected piglet diarrhea (Gao et al., 2020). In this study, we used RNA sequencing (RNA-seq) to perform transcriptome analysis of the CPB2 and control groups of IPEC-J2 cells and to identify differentially expressed lncRNAs in response to CPB2. We also analyzed the gene ontology (GO) enrichment of differential lncRNAs and carried out Kyoto Encyclopedia of Genes and Genomes (KEGG) pathway analysis with the aim of identifying possible molecular mechanisms of CPB2 toxin-induced diarrhea in piglets. We identified a key lncRNA, lncRNA *EN-90756*, which was highly expressed in CPB2-induced IPEC-J2 cells and applied a series of biological experiments to explore its regulatory mechanism. These results increase our understanding of the molecular mechanisms of lncRNAs in CPB2 toxin-induced diarrhea in piglets.

2. Materials and methods

2.1. Preparation and purification of the CPB2 toxin

The CPB2 toxin was extracted and purified according to Luo's method (Luo et al., 2020). Briefly, a recombinant plasmid containing the CPB2 gene, pET-28a-CPB2, was constructed and transformed into BL21 *E. coli* cells for expression. The expressed CPB2 protein was purified using High Affinity Ni-Charged Resin FF (GenScript, Nanjing, China) and concentrated using PEG6000. Finally, a ToxOut™ Rapid Endotoxin Removal Kit (AmyJet Scientific, Wuhan, China) was used to remove the endotoxin.

2.2. Cell culture and processing

Intestinal porcine epithelial cell line-J2 cells were provided by the BeNa Culture Collection (Beijing, China). Cells were cultured using Dulbecco's modified Eagle's medium (HyClone, Logan, UT, USA) containing 10% fetal bovine serum (Gibco, Grand Island, NY, USA) and 1% double antibiotics (penicillin

and streptomycin) at 37°C in an atmosphere of 5% CO₂. The CPB2 group of cells was treated with the CPB2 toxin (20 µg/ml). Three replicates were set up for each group.

2.3. RNA-sequencing (RNA-seq) and data analysis

Total RNA was extracted from the control and CPB2-treated cells using RNAiso™ Reagent (Invitrogen, Carlsbad, CA, USA). The total RNA quantity and purity were assessed using a Bioanalyzer 2100 and RNA 1000 Nano LabChip Kit (Agilent, Santa Clara, CA, USA), respectively. The RNA samples were of high quality with RNA integrity numbers > 7. Ribosomal RNA was removed using a Ribo-Zero™ rRNA Removal Kit (Illumina, San Diego, CA, USA) and then reverse transcribed into cDNA. The cDNA libraries were constructed and sequenced on an Illumina NovaSeq™ 6000 platform (Illumina, San Diego, CA, USA) using 2 × 150 bp paired-end sequencing. The raw data obtained from IPEC-J2 samples were stored in the NCBI SRA database (accession number: PRJNA749943).

The raw data were processed using FastQC software.¹ This step produced clean data by removing the reads with shifted connectors and low quality sequences (quality score < Q30). The reads were mapped against the pig genome assembly (*Sscrofa* 11.1) and the alignment results were assessed using HISAT2² (Kim et al., 2015). StringTie software³ was used to estimate gene expression levels according to fragments per kilobase of transcript per million mapped reads (FPKM) (Trapnell et al., 2010). After all transcripts were obtained, transcripts smaller than 200 bp and known mRNAs were removed and lncRNA prediction was performed on the remaining transcripts using CPC, Pfam-sca, and CNCI (Kong et al., 2007; Sun et al., 2013). LncRNAs with fold change (FC) ≥ 2 and *p* < 0.05 were regarded as significantly differentially expressed.

Long non-coding RNA target genes were predicted using both *cis* and *trans* methods. LncRNA *cis*-regulatory target genes were mainly predicted based on positional relationships. The mRNAs that were differentially expressed within 100 kb upstream and downstream of the lncRNA were considered to be lncRNA *cis*-regulatory target genes. The *trans*-regulated target genes of lncRNAs were analyzed using RIsSearch (Wenzel et al., 2012) software. Screening conditions included the formation of secondary structure free energy between the lncRNA and mRNA sequences (energy < -11) and the Pearson correlation coefficient (*r* > 0.95 or *r* < -0.95). Subsequently, GOSeq Release 2.12 and KO-BAS (V2.0)

(Kanehisa et al., 2007; Young et al., 2010) were used to perform GO and KEGG pathway enrichment analyses of the target genes of the lncRNAs, respectively.

2.4. Quantitative real-time reverse transcription polymerase chain reaction (qRT-PCR)

Total RNA was extracted from IPEC-J2 cells (1×10^7) according to the method described in section “2.3 RNA-sequencing (RNA-seq) and data analysis.” Cytoplasmic and nuclear RNAs of IPEC-J2 cells were isolated using a PARIS™ Kit reagent kit (Ambion, Austin, TX, USA) according to the instructions provided by the supplier. Total RNA was reverse transcribed into cDNA using Evo M-MLV Mix Kit with gDNA Clean for qPCR AG11728 (Accurate Biotechnology, Hunan, China). The qRT-PCR assay was performed according to the instructions of SYBR Green assay (Accurate Biotechnology, Hunan, China) and performed on a Roche LightCycler 480 (Roche Applied Science, Mannheim, Germany). Gene expression levels were normalized to that encoding glyceraldehyde-3-phosphate dehydrogenase (*GAPDH*) to determine the relative expression using the $2^{-\Delta\Delta Ct}$ method (Ljvak, 2001). The PCR primers for transcripts and genes are listed in Table 1.

2.5. Single RNA fluorescent *in situ* hybridization (FISH)

The green fluorescent FAM-labeled probe for lncRNA *EN-9075* (lncRNA-FISH probe mix) was designed by GenePharma (Shanghai, China) and detected using a fluorescent *in situ* hybridization kit (GenePharma) according to the manufacturer's instructions. In short, IPEC-J2 cells were inoculated overnight in 48-well plates at a density of 1×10^4 cells/well and then treated with CPB2 toxin for 24 h. IPEC-J2 cells were then fixed with 4% (v/v) paraformaldehyde for 15 min at room temperature. The IPEC-J2 cells permeabilized in phosphate-buffered saline (PBS) containing 0.1% Triton X-100 for 15 min at room temperature and then blocked with pre-hybridization buffer for 30 min at 37°C. The IPEC-J2 cells were treated with the FAM-labeled probe in hybridization buffer (10 µL, 10 µM probe, and 90 µL hybridization buffer) the dark at 37°C for 14 h. The cells were then washed three times with wash buffer (4 × SSC/2 × SSC) in the dark and stained with 4',6-diamidino-2-phenylindole for 15 min. The IPEC-J2 cells were washed three times with PBS and then observed under a fluorescent microscope at 200× magnification (Olympus IX71, Tokyo, Japan).

1 www.bioinformatics.babraham.ac.uk/projects/fastqc/

2 ccb.jhu.edu/software/hisat2/

3 ccb.jhu.edu/software/stringtie/

TABLE 1 Quantitative real-time reverse transcription polymerase chain reaction (qRT-PCR) primers for amplifying specific genes.

GeneID/Gene name		Nucleotide sequence (5'–3')	Product length (bp)
ENSSSCG00000041190	Forward	GAATCTGAACTTCTTGCCACA	112
	Reverse	TACTAACATTCCCTGCCCAT	
ENSSSCG00000047438	Forward	CATTATGTGCCACCGACGAA	178
	Reverse	TCACTGAAAGCCAAGTGTC	
ENSSSCG00000046898	Forward	TTTATTTGGAAGCGACCCT	110
	Reverse	TCCCCTCATTCTCAGAGTCG	
ENSSSCG00000045823	Forward	CCTTGCCTCACTCGGTGT	239
	Reverse	GGATCCTATGCAGCAACCC	
LOC106507243	Forward	CGGCGCTTACAGACTCC	143
	Reverse	GGCTCCAGGAACAAGTACCC	
LOC102162336	Forward	GCCCATCCCTTGAAAATGACGA	157
	Reverse	CCGCCCTTCTCAACACC	
ENSSSCG00000041166	Forward	GAAACGAATCTGACTAGCACCC	165
	Reverse	TAATCCCTGGCCTCACTCGG	
ENSSSCG00000047080	Forward	CCCCGACCTGATAAGTCCT	105
	Reverse	AGGCCATCTTCCTAATCCCT	
LOC106508476	Forward	GGAAACAGCCTAAATGGTCA	160
	Reverse	GGCCTCATGTAACAAGGACTCA	
ENSSSCG00000048701	Forward	AGACTCTGACGTGGTAGGACA	145
	Reverse	TTGGAGAAGTGTACACCCGT	
U6	Forward	TTATGGGTCTAGCCTGAC	224
	Reverse	CACTATTGCGGGTCTGC	
MX1	Forward	CCACCTGAAGAAGGGCTAC	219
	Reverse	AACAGGGGCAGAGTTTAC	
GAPDH	Forward	AGTATGATCCACCCACGGC	139
	Reverse	TACGTAGCACCAGCATCACC	
Caspase 3	Forward	CCGAAATGTTTGCTGACGGC	152
	Reverse	CCGATCTCGAAGGAAGTCCA	
Caspase 8	Forward	CGGCTCTGAGCAAGACCTTTA	173
	Reverse	GCCGTAGATGATGCCCTTGT	

2.6. Cell transfection

The small interfering RNA targeting lncRNA *EN-90756* (si EN-90756) and the negative control siRNA (si NC) were obtained from GenePharma. IPEC-J2 cells (1×10^5 cells/ml) were grown overnight in six-well plates until they were 70% confluent for transfection. Lipofectamine 2000 (Invitrogen) was mixed with Opti-MEM medium (Invitrogen, CA, USA) and left for 5 min. Then, the solution was added to si EN-90756, si NC (1:1 ratio) diluted with Opti-MEM medium, mixed and left for 20 min. The prepared mixtures were added to IPEC-J2 cells separately and transfection was completed after 24 h.

2.7. Cell viability and proliferation assay

Intestinal porcine epithelial cell line-J2 (density of 5×10^3 /well) were seeded in 96-well plates, with three replicates for each group. After treatment with CPB2 toxin, cell viability was determined according to the instructions of Cell Counting Kit-8 (Beyotime, Shanghai, China). IPEC-J2 cells (1×10^5 cells/ml) were grown in six-well plates and treated with CPB2 toxin or PBS. Cell proliferation was assayed using the BeyoClick™ EdU Cell Proliferation Kit with Alexa Fluor 488 [5-ethynyl-2'-deoxyuridine (EdU), Beyotime]. Cell proliferation was observed under a fluorescence microscope at 200× magnification (Olympus IX71).

2.8. Flow cytometry

Intestinal porcine epithelial cell line-J2 cells (1×10^5 cells/ml) were grown in six-well plates, transfected with si NC or si EN-90756 for 24 h and then treated with CPB2 toxin for 24 h. Cells were collected and washed twice with PBS. Then, 1 ml of pre-cooled 70% ethanol was added to the cells, mixed with gentle shaking, and fixed at 4°C for 12 h. The ethanol was discarded, the cells were washed using PBS and collected by centrifugation. Then, the cells were incubated with Annexin V-fluorescein isothiocyanate and propidium iodide for 20 min at 25°C in the dark. Apoptosis was detected using a FACSCalibur flow cytometer (BD Biosciences, San Jose, CA, USA).

2.9. Mitochondrial membrane potential assay

Intestinal porcine epithelial cell line-J2 cells were transfected with si NC or si EN-90756 and treated with CPB2 toxin or PBS and then assayed for mitochondrial membrane potential ($\Delta\psi_m$) according to the instructions of the mitochondrial

membrane potential assay kit with JC-1 (Beyotime). Briefly, cells were incubated with JC-1 staining solution at 37°C for 20 min, washed two times with JC-1 staining buffer (1×) and then observed under a fluorescent microscope (Olympus IX71).

2.10. Western blotting

Total IPEC-J2 cell proteins were extracted using Radioimmunoprecipitation assay (Beyotime). The extracted proteins were quantified using a bicinchoninic acid protein analysis kit (Beyotime). Sodium dodecyl sulfate-polyacrylamide gel electrophoresis (12%) was used to separate equal amounts of proteins, which were then transferred to polyvinylidene fluoride membranes (Millipore, Billerica, MA, USA). The membranes were incubated with primary antibodies overnight at 4°C.

The primary antibodies comprised those recognizing: MX dynamin like GTPase 1 (MX1) (bsm-51528m, Bioss, Woburn, MA, USA; 1:1,000); Janus kinase 1 (JAK1) (bs-1439R, Bioss; 1:1,000); phosphorylated (p-JAK1) (bs-3238R, Bioss; 1:1,000); signal transducer and activator of transcription 3 (STAT3) (GB11176, Servicebio, Wuhan, China; 1:1,000); p-STAT3 (bs-1658R, Bioss; 1:1,000); and GAPDH (GB15002, Servicebio;

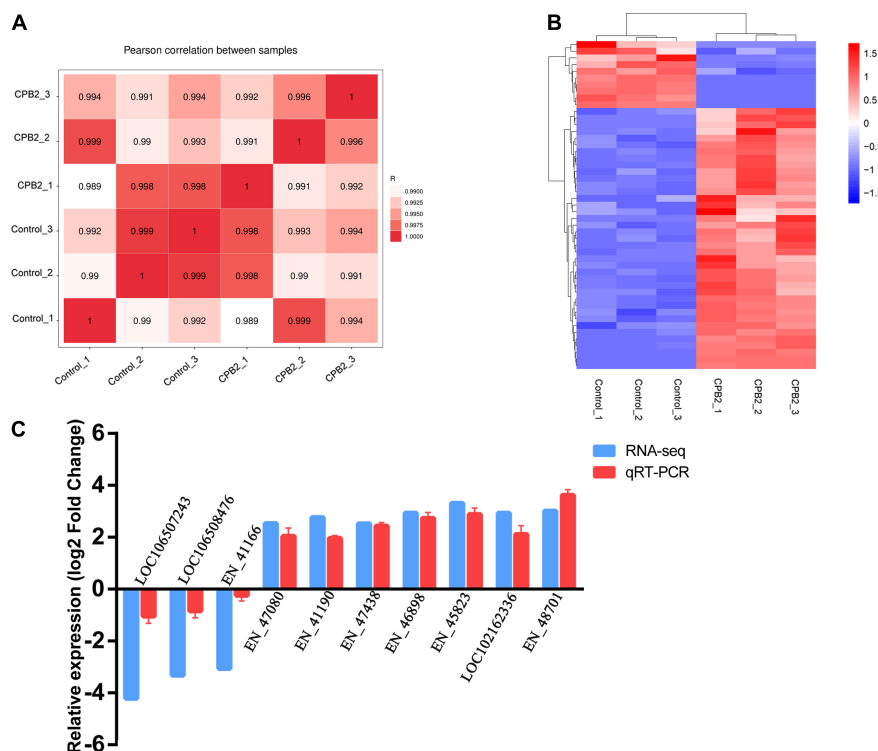


FIGURE 1

Quality analysis of the RNA-seq data. (A) Chart of the expression correlation between samples. *R* is Pearson's correlation coefficient. (B) A hierarchical heat map of differential long non-coding RNAs (lncRNAs) in the control and toxin-treated intestinal porcine epithelial cell line-J2 (IPEC-J2) cells. Data are expressed as the fragments per kilobase of transcript per million mapped reads. Different colors indicate different levels of gene expression, with colors ranging from blue through white to red indicating low to high expression. (C) Quantitative real-time reverse transcription polymerase chain reaction (qRT-PCR) validation of 10 differentially expressed lncRNAs.

1:2,000). After incubation with horseradish peroxidase-labeled secondary antibodies (GB23303, Servicebio; 1:5,000) or (GB25301, Servicebio; 1:5,000), the immunoreactive protein bands were observed using the enhanced chemiluminescence method (Thermo Fisher Scientific, Waltham, MA, USA).

2.11. Statistical analysis

The results were statistically analyzed using SPSS v.21 software (IBM Corp., Armonk, NY, USA). All experiments had three replicates, and the experimental data are expressed as the mean \pm standard deviation (SD). Differences were determined using Student's *t*-test (two-tailed test). *P*-values < 0.05 were considered statistically significant.

3. Results

3.1. Quality analysis of the RNA-seq data

Six cDNA libraries of IPEC-J2 cells from the control and CPB2 groups were sequenced and Pearson's correlation coefficient between the two groups ranged from 0.98 to 0.99, indicating a high degree of similarity in expression patterns between the samples from the same group (Figure 1A). After quality control of the raw data, we obtained approximately 8.36 Gb of high quality data and the average GC content of the six libraries was approximately 53%; and the Q30 (sequencing error rate less than 0.001) per sample ranged from 95.34 to 96.14% (Supplementary Table 1). Over 70% of the clean reads were mapped to the porcine reference genome, containing approximately 60% of the unique mappings (Supplementary Table 2).

3.2. Identification of differentially expressed lncRNAs

A total of 6,558 lncRNAs were identified in IPEC-J2 cells in the control and CPB2 groups, among which 39 were significantly up-regulated and 10 were significantly down-regulated lncRNAs between the two groups of IPEC-J2 cells [*p*-value < 0.05 and $|\log_2(\text{FC})| \geq 1$] (Figure 1B and Supplementary Table 3).

Ten significantly differentially expressed lncRNAs were randomly selected for qRT-PCR validation of the accuracy of the sequencing results. The expression levels of lncRNAs *LOC106507243*, *LOC106508476*, and *EN-41166* were down-regulated after CPB2 treatment, while lncRNAs *EN-47080*, *EN-41190*, *EN-47438*, *EN-46898*, *EN-45823*, *LOC102162336*, and *EN-48701* were up-regulated after CPB2 treatment (Figure 1C). The results of qRT-PCR were consistent with the RNA-seq

results, demonstrating that the sequencing results were reliable and reproducible.

3.3. GO terms and KEGG pathways analysis of lncRNA EN-90756 target gene

To explore their functions, the 49 differentially expressed lncRNAs were subjected to target gene prediction. Consequently, genes associated with the immune response and viral defense (e.g., *CXCL2*, *MX1*, *OASL*) were identified among the target genes (Figure 2A) of the significantly differentially expressed lncRNA *EN-90756*. Further enrichment analysis revealed that significantly enriched GO terms were defense response to virus, negative regulation of viral genome replication, negative regulation of apoptotic process, and regulation of cell cycle (Figure 2B). The KEGG enrichment analysis identified Legionellosis, influenza A, Salmonella infection, and cellular senescence signaling pathways were significantly enriched (Figure 2C). Interestingly, the *MX1* gene was enriched in the defense response to virus, cellular response to type I interferon, and hepatitis C, influenza A, and measles signaling pathways. These results suggest that lncRNA *EN-90756* might be involved in the invasion of IPEC-J2 cells by CPB2 toxin through the regulation of target genes.

3.4. LncRNA EN-90756 was highly expressed in CPB2-treated IPEC-J2 cells

The expression pattern of lncRNA *EN-90756* in CPB2-treated cells was determined at different time points (0, 12, 24, and 36 h) of CPB2 toxin treatment. The results showed that lncRNA *EN-90756* expression was significantly up-regulated during CPB2 toxin treatment and reached its highest level at 24 h (Figure 3A). The nuclear/cytosol separation assay showed that lncRNA *EN-90756* was mainly located in the cytoplasm, with a small amount in the nucleus (Figure 3B). RNA-FISH results also confirmed that the green fluorescent signal of lncRNA *EN-90756* was distributed in both the nucleus and the cytoplasm, but was mainly located in the cytoplasm (Figure 3C). These results suggest that lncRNA *EN-90756* might be an important regulator in the regulation of *C. perfringens* type C infection.

3.5. Knockdown of lncRNA EN-90756 inhibited the proliferation of IPEC-J2 cells

Long non-coding RNA *EN-90756* was knocked down to investigate its role in CPB2-treated IPEC-J2 cells. The expression

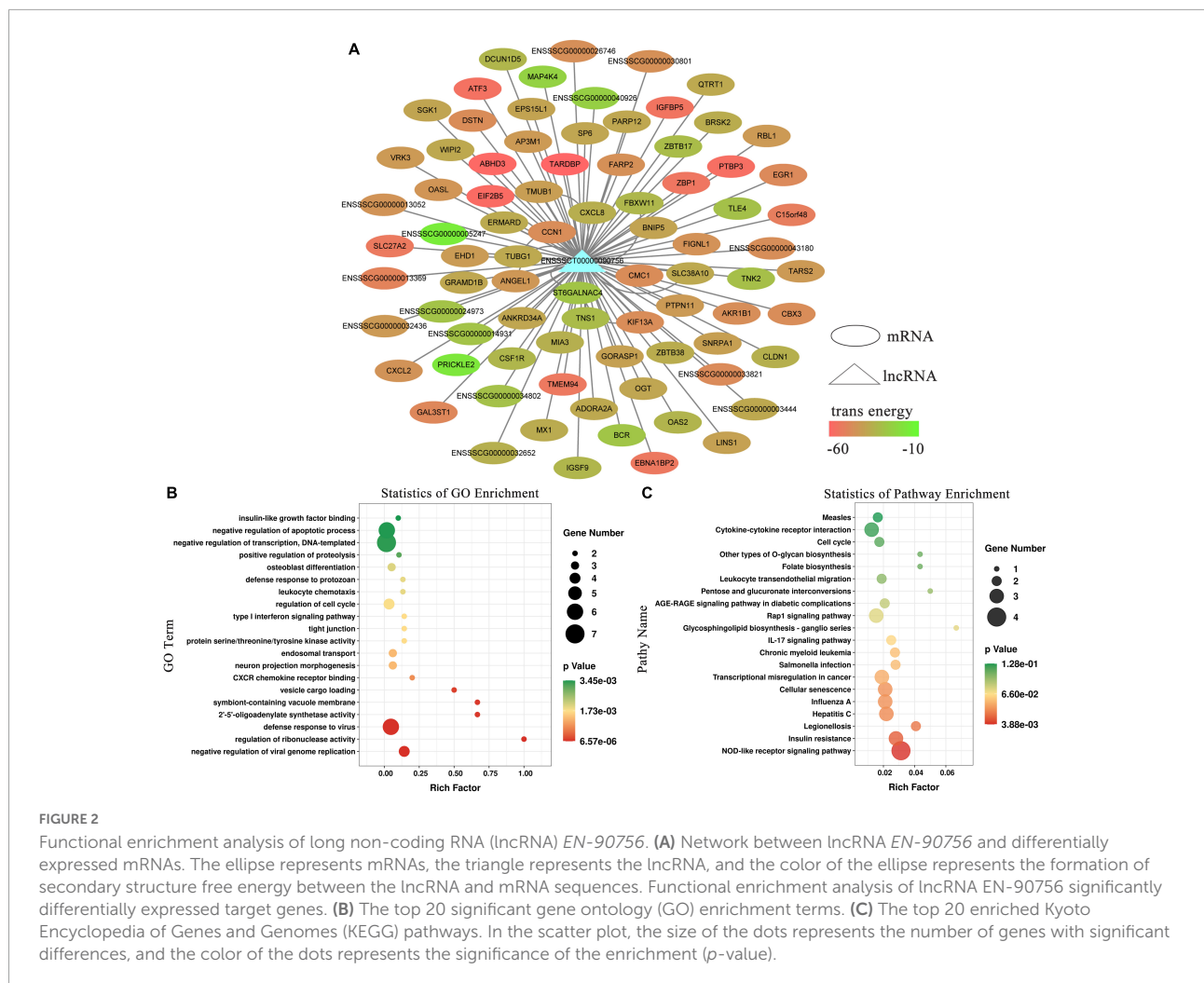


FIGURE 2
 Functional enrichment analysis of long non-coding RNA (lncRNA) *EN-90756*. **(A)** Network between lncRNA *EN-90756* and differentially expressed mRNAs. The ellipse represents mRNAs, the triangle represents the lncRNA, and the color of the ellipse represents the formation of secondary structure free energy between the lncRNA and mRNA sequences. Functional enrichment analysis of lncRNA *EN-90756* significantly differentially expressed target genes. **(B)** The top 20 significant gene ontology (GO) enrichment terms. **(C)** The top 20 enriched Kyoto Encyclopedia of Genes and Genomes (KEGG) pathways. In the scatter plot, the size of the dots represents the number of genes with significant differences, and the color of the dots represents the significance of the enrichment (p-value).

level of lncRNA *EN-90756* was significantly reduced after transfection with si *EN-90756* (Figure 4A). Cell viability assays showed that knockdown of lncRNA *EN-90756* in CPB2-treated IPEC-J2 cells significantly reduced cell viability (to 78.75%) (Figure 4B). EdU analysis revealed that more EdU-positive cells were observed in the CPB2 and si NC + CPB2 groups, while fewer EdU-positive cells were observed in the si *EN-90756* + CPB2 group (Figures 4C, D). These results indicated that down-regulation of lncRNA *EN-90756* inhibited the proliferation of IPEC-J2 cells.

3.6. Knockdown of lncRNA *EN-90756* promoted apoptosis in IPEC-J2 cells

JC-1 staining showed that after knocking down lncRNA *EN-90756*, the fluorescence turned almost entirely green in CPB2-treated IPEC-J2 cells, reflecting the collapse of the $\Delta\psi_m$ (Figure 5A). This suggested that knockdown of lncRNA *EN-90756* exacerbated CPB2-induced loss of $\Delta\psi_m$ in IPEC-J2

cells. Caspase 3 and Caspase 8, are key proteins in apoptosis, and qRT-PCR revealed that the mRNA expression levels of *Caspase 3* and *Caspase 8* were significantly elevated in CPB2-induced IPEC-J2 cells after knockdown of lncRNA *EN-90756* (Figures 5B, C). Furthermore, the results of flow cytometry showed that the apoptosis rate was 27.35% in the CPB2 group and 37.74% in the si *EN-90756* + CPB2 group (Figure 5D). These results suggested that down-regulation of lncRNA *EN-90756* promoted apoptosis in IPEC-J2 cells.

3.7. Knockdown of lncRNA *EN-90756* promoted MX1 expression and inhibited the JAK-STAT signaling pathway

Long non-coding RNA *EN-90756* knockdown resulted in significant up-regulation of the expression of target gene *MX1*

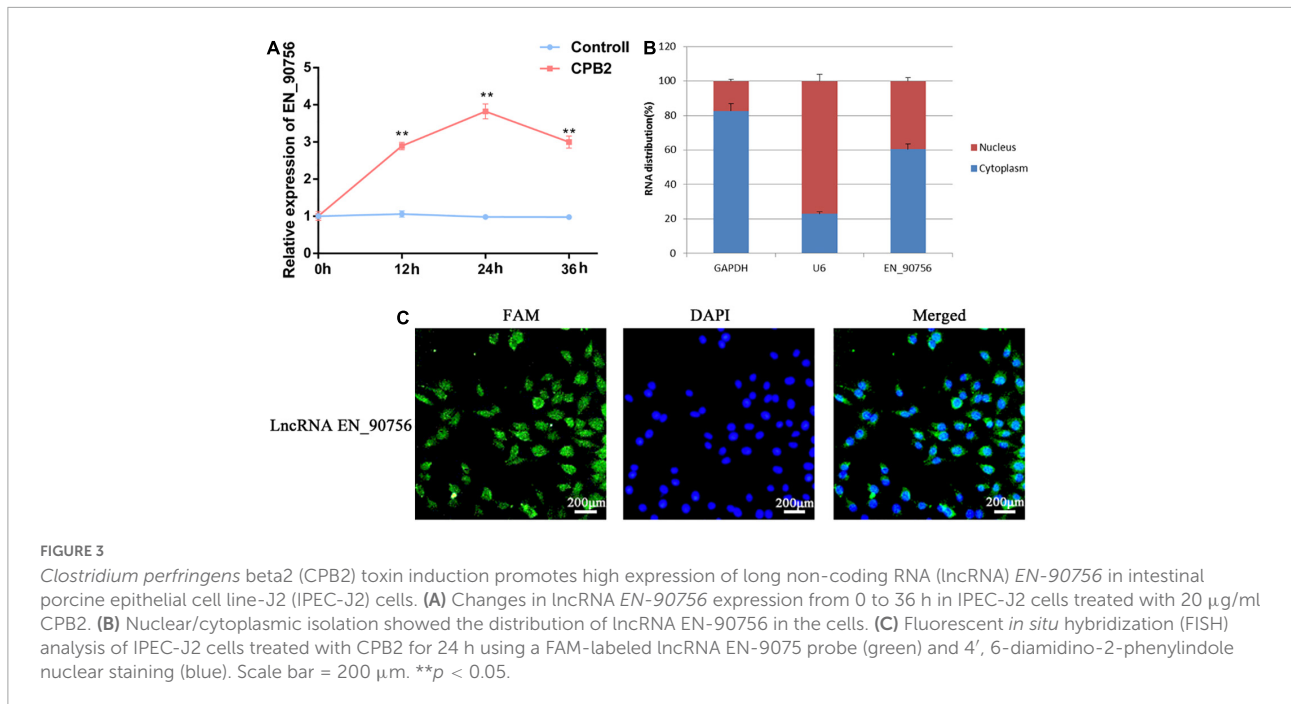


(Figure 6A) and its protein level (Figures 6B, C) in CPB2-induced IPEC-J2 cells. The JAK-STAT signaling pathway is involved in a variety of important biological processes, including cell proliferation and apoptosis. To explore the effect of lncRNA *EN-90756* on the JAK-STAT pathway, we examined the levels of JAK1 and STAT3 proteins and their phosphorylation. The results showed that JAK1 and p-JAK1 protein levels were significantly down-regulated in CPB2-induced IPEC-J2 cells after knockdown of lncRNA *EN-90756*. STAT3 and p-STAT3 proteins were barely detected in CPB2-induced IPEC-J2 cells after knockdown of lncRNA *EN-90756* (Figures 6D, E). The results suggested that lncRNA *EN-90756* regulates *MX1* expression and affects JAK-STAT pathway activation in CPB2-induced IPEC-J2 cells.

4. Discussion

Clostridium perfringens causes enteritis and enterotoxaemia in domestic animals, wildlife and humans, and its virulence is mainly due to its ability to produce toxins. CPB2 toxin is an important pathogenic factor causing necrotizing enteritis in animals. The correlation between neonatal piglet diarrhea and the presence of *C. perfringens* capable of producing CPB2 toxin in their intestine is extremely high (Bueschel et al., 2003). To further investigate the effects of CPB2 toxin on animal diarrhea, CPB2 toxin protein was isolated and purified. CPB2 toxin protein was moderately cytotoxic to human NCM460 intestinal epithelial cells (Zeng et al., 2016); and induced apoptosis and inflammation in porcine small intestinal epithelial cells, impairing the intestinal barrier function (Gao et al., 2020).

However, the effects of host lncRNAs in CPB2 toxin-treated IPEC-J2 cells and how they are regulated are unclear. Here, IPEC-J2 cells from the CPB2 and control groups were analyzed using RNA-seq to search for lncRNAs affected by CPB2 toxin and to explore the function of these lncRNAs, which will inform studies on the effects of CPB2 toxin on piglet diarrhea.

Long non-coding RNAs have emerged as important regulators of various biological processes and diseases, interacting with other molecules and thus participating in the regulation of histone modifications, gene transcription, RNA stability, RNA splicing, and transcriptional or translational modifications. lncRNA *PVT1* promotes cancer initiation and progression by acting as a competing endogenous RNA (ceRNA), activating STAT3 signaling or KAT2A acetyltransferase, or interacting with myelocytomatosis oncogene (MYC) (Zhao J. et al., 2018; Jin et al., 2019; Sun et al., 2019). Systemic loss-of-function experiments demonstrate that long intergenic ncRNAs (lincRNAs) are involved in the molecular circuitry of embryonic stem cells and are required for the maintenance of embryonic stem cell pluripotency (Guttman et al., 2011). In recent years, numerous studies related to lncRNAs have been conducted in domestic animals. The 73 up-regulated and 68 down-regulated differentially expressed lncRNAs were identified in placentas from Meishan pigs at the establishment and expansion stages of placental fold development, and these differential lncRNAs were associated primarily with the placental fold development process (Deng et al., 2020). In the present study, we detected 49 significantly differentially expressed lncRNAs between control IPEC-J2 cells and CPB2 treated cells. The target genes of significantly different lncRNA *EN-90756* were mainly associated with

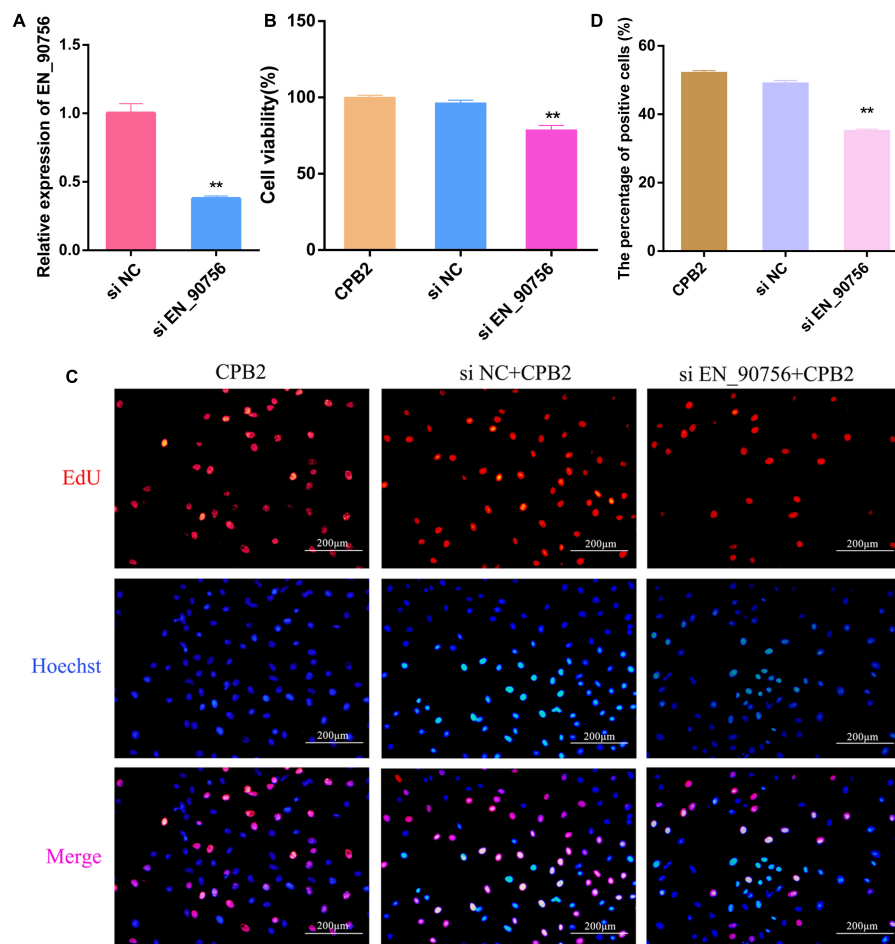


FIGURE 4

Knockdown of long non-coding RNA (lncRNA) *EN-90756* inhibits the proliferation of intestinal porcine epithelial cell line-J2 (IPEC-J2) cells. (A) Expression of lncRNA *EN-90756* in *Clostridium perfringens* beta2 (CPB2) cells after transfection with si NC and si *EN_90756*. (B) Effect of lncRNA *EN-90756* on the viability of CPB2-treated IPEC-J2 cells. (C) si NC or si *EN_90756* were transfected into CPB2-treated IPEC-J2 cells, followed by staining with 5-ethynyl-2'-deoxyuridine (EdU) (red) for DNA replication and Hoechst (blue) for nuclei. Scale bar = 200 μ m. (D) The percentages of EdU-positive cells. ** $p < 0.05$.

defense responses to viruses, suggesting a possible regulatory role of lncRNA *EN-90756* in CPB2-treated cells.

Aberrant lncRNA expression is implicated in the pathogenesis of many diseases. Highly expressed lncRNA *LINC00707* mediates a range of biological functions in humans, including cell proliferation, apoptosis, metastasis, invasion, cell cycle arrest, inflammation, and even osteogenic differentiation (Yao et al., 2022). In present study, the expression of lncRNA *EN-90756* was significantly up-regulated with increasing treatment time of CPB2 toxin and reached its highest value at 24 h. EdU and cell viability assays showed that knockdown of lncRNA *EN-90756* inhibited the proliferation of CPB2-treated IPEC-J2 cells.

The $\Delta\Psi$ m plays a crucial role in many biological processes and is highly correlated with apoptosis (Tian et al., 2019). In epithelial cancer cells, $\Delta\Psi$ m is often abnormally higher

than that in normal cells, which is associated with increased invasiveness of cancer cells *in vitro* and their increased metastatic potential *in vivo* (Begum et al., 2021). Instability of the $\Delta\Psi$ m leads to early reperfusion arrhythmias and systolic dysfunction (Ashok et al., 2020). Treatment with isoliquiritigenin increased apoptosis in human bladder cancer T24 cells in a concentration-dependent manner and caused a decrease in the $\Delta\Psi$ m in a time-dependent manner (Si et al., 2017). It has been reported that $\Delta\Psi$ m decreased in CPB2-treated IPEC-J2 cells (Luo et al., 2020). Here, we noted that knockdown of lncRNA *EN-90756* resulted in a significant decrease in the $\Delta\Psi$ m in IPEC-J2 cells, implying that the cells entered an early apoptotic phase. Initiator caspases (such as Caspase 8) are involved in early apoptotic signaling, and once Caspase 8 is activated, it can immediately initiate downstream effector caspases (e.g., Caspase 3) to promote

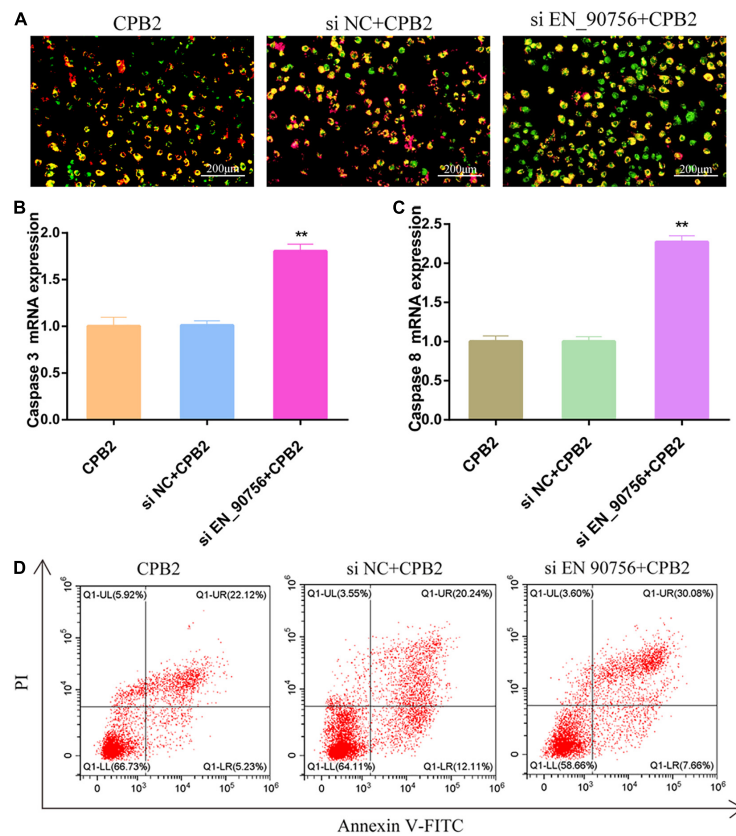


FIGURE 5

Knockdown of long non-coding RNA (lncRNA) *EN-90756* promoted apoptosis in intestinal porcine epithelial cell line-J2 (IPEC-J2) cells. (A) The $\Delta\psi_m$ was detected in IPEC-J2 cells treated with *Clostridium perfringens* beta2 (CPB2) for 24 h and stained using the JC-1 probe. Scale bar = 200 μ m. The shift from red to green fluorescence represents a decrease in cell membrane potential. The mRNA expression of *caspase 3* (B) and *caspase 8* (C) in cells treated with 20 μ g/ml CPB2 toxin for 24 h. (D) Apoptosis was detected using Annexin V-fluorescein isothiocyanate. ** $p < 0.05$.

apoptosis (O'Donnell et al., 2011; Willson, 2019; Zhaojun et al., 2022). We found that CPB2-induced the mRNA expression of apoptotic proteins *Caspase 3* and *Caspase 8* in IPEC-J2 cells, which was significantly increased after lncRNA *EN-90756* inhibition. Meanwhile, flow cytometry showed that down-regulation of lncRNA *EN-90756* expression promoted apoptosis in IPEC-J2 cells. In summary, knockdown of lncRNA *EN-90756* promoted apoptosis in CPB2-induced IPEC-J2 cells.

The localization of lncRNAs is closely related to their mode of regulation. Although most lncRNAs are transcribed by RNA polymerase II (Pol II) and have polyadenylate tails and m7G cap structures, they are processed and spliced less efficiently and exhibit significant cytosolic localization (Derrien et al., 2012; Tian and Manley, 2017; Guo et al., 2020). When localized in the nucleus, lncRNAs can interact with a variety of molecules such as DNA, RNA, and proteins to regulate chromosome structure and function, or regulate gene transcription in *cis* or *trans*, affecting mRNA splicing, stabilization, and translation (Fanucchi et al., 2019; Statello et al., 2020). lncRNAs localized in the cytoplasm are mainly

involved in the regulation of gene expression in *trans* at the post-transcriptional level, such as the regulation of mRNA translation and degradation, or in the regulation of intracellular signaling pathways (Hartford and Lal, 2020). Special organelle-localized lncRNAs are involved in organelle function and metabolic regulation, such as the mitochondrial oxidative response and homeostatic balance (Mercer et al., 2011; Carlevaro-Fita et al., 2016; Noh et al., 2016). FISH analysis showed that lncRNA *EN-90756* was distributed in both the nucleus and cytoplasm, suggesting that lncRNA *EN-90756* may be involved in post-transcriptional regulation. lncRNA *TINCR* regulates the stability of *KRT80* by binding to *STAU1* protein, thereby affecting epidermal cell differentiation (Kretz et al., 2013). The lncRNA *AS Uchl1* controls the translation of *Uchl1* via an embedded *SINEB2* repeat sequence (Carrieri et al., 2012, 2015). No neighboring genes were found in the vicinity of lncRNA *EN-90756*, suggesting that lncRNA *EN-90756* may function by regulating distal target genes. To further investigate the regulatory role of lncRNA *EN-90756* in IPEC-J2 cells, we examined significantly differentially expressed

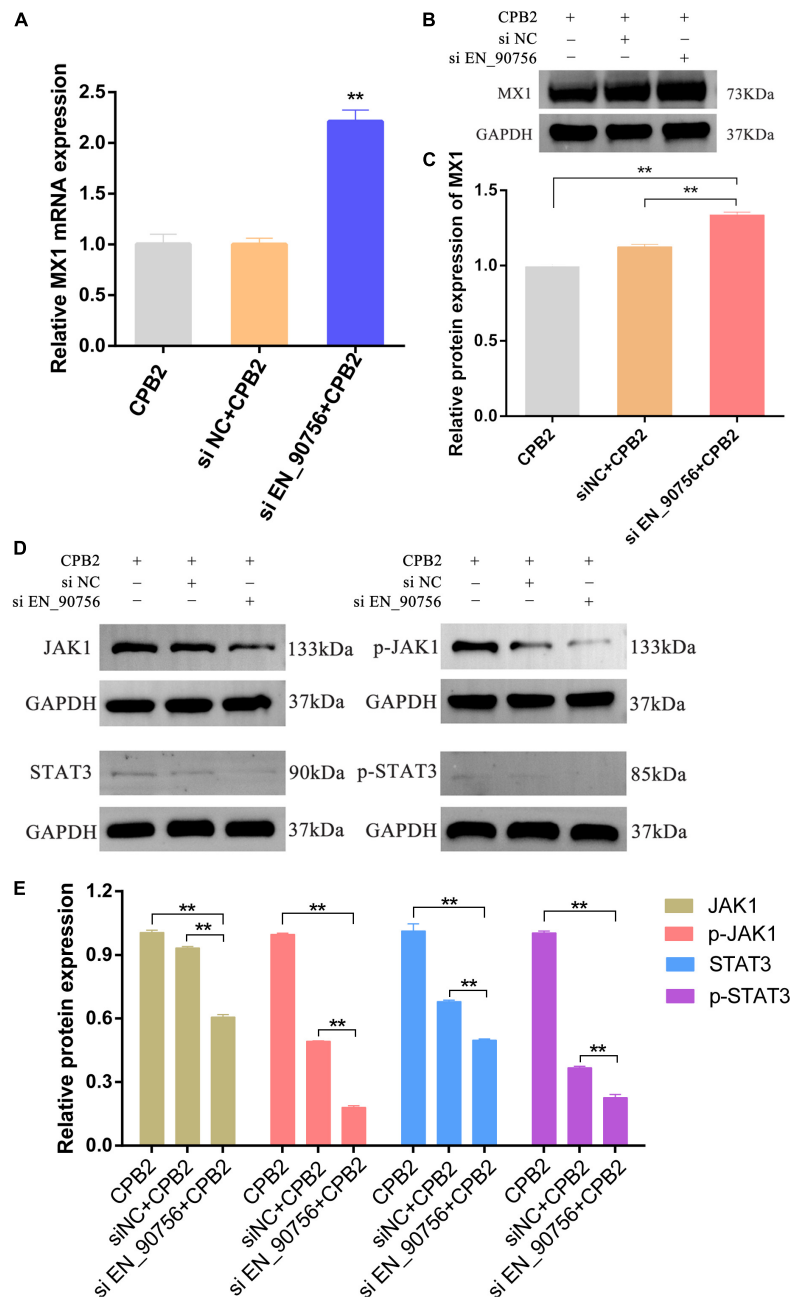


FIGURE 6
 Inhibition of long non-coding RNA (lncRNA) *EN-90756* promoted MX1 expression and suppressed the Janus kinase (JAK)-signal transducer and activator of transcription (STAT) signaling pathway. The mRNA expression (A) and protein levels (B,C) of the target gene MX1 in *Clostridium perfringens* beta2 (CPB2)-induced intestinal porcine epithelial cell line-J2 (IPEC-J2) cells before and after lncRNA *EN-90756* inhibition. (D,E) Western blotting analysis of JAK1, p-JAK1, STAT3, and p-STAT3 protein levels in IPEC-J2 cells after CPB2 stimulation by lncRNA *EN-90756* inhibition. ***p* < 0.05.

target genes. We noted a significant up-regulation of MX1 expression after lncRNA *EN-90756* knockdown. *MX1* is an interferon-stimulated gene that plays a role in the defense of mammalian cells against influenza A and other viruses by repressing viral gene transcription (Pavlovic et al., 1992; Holzinger et al., 2007; Raftery and Stevenson, 2017; Spitaels

et al., 2019). *MX1* represents a key component of the mouse innate immune system that protects mice from the highly lethal human H5N1 influenza virus (Tumpey et al., 2007). lncRNA *IVRPIE* promoted the host immune response against influenza A virus by regulating the expression of interferon β 1 and *MX1* (Zhao et al., 2020). These results suggest that lncRNA

EN-90756 might influence the immune response of IPEC-J2 cells by regulating MX1 expression, providing clues for disease resistance breeding and disease treatment in piglet diarrhea.

Previous studies confirmed that the JAK/STAT pathway plays an important role in mediating cell fate such as apoptosis, differentiation, and proliferation (Muoz-Cánoves et al., 2013; Richard and Stephens, 2014; O'Shea et al., 2015; Jia et al., 2016). The JAK family of receptor-associated tyrosine kinases act as primary transducers of multiple cytokine receptors and mediate a variety of their effects through the phosphorylation of STAT transcription factors (Derecka et al., 2012; Lee et al., 2016). LncRNA *FEZFI-AS1* promotes proliferation and inhibits apoptosis in ovarian cancer through activation of the JAK-STAT3 pathway (Zhao X. et al., 2018). Crizotinib could promote cell apoptosis of human lung cancer cell line H2228 by regulating the expression of JAK and STAT proteins in the JAK-STAT signaling pathway (Lu et al., 2018). LncRNA *MEG3* inhibited the migration of oral squamous cell carcinoma cells and promoted apoptosis by regulating the JAK-STAT pathway (Tan et al., 2019). Previous studies have shown that CPB2 toxin treatment of IPEC-J2 cells inhibits cell proliferation, promotes apoptosis, and accelerates the inflammatory response (Gao et al., 2020; Luo et al., 2020; Yang et al., 2022). Here, lncRNA *EN-90756* was able to alleviate CPB2 toxin-induced apoptosis and promote cell proliferation in IPEC-J2 cells. In addition, the JAK-STAT signaling pathway was regulated by lncRNA *EN-90756*, as inferred from the expression levels of related proteins. The above results suggested that lncRNA *EN-90756* might regulate the proliferation and apoptosis of IPEC-J2 cells by affecting the JAK-STAT pathway. However, the regulation of lncRNA is complex and the specific mechanism of regulation of JAK-STAT by lncRNA *EN-90756* needs to be further investigated.

In conclusion, this study identified differentially expressed lncRNAs in the CPB2 and control groups of IPEC-J2 cells. In addition, we found that CPB2 toxin treatment promoted significant differential lncRNA *EN-90756* expression up-regulation. Inhibition of lncRNA *EN-90756* suppressed the proliferation of CPB2-treated IPEC-J2 cells and promoted apoptosis. Mechanistically, lncRNA *EN-90756* might affect the antiviral ability of IPEC-J2 cells by regulating the expression of MX1. Meanwhile, lncRNA *EN-90756* might regulate CPB2-induced cell proliferation and apoptosis by affecting the JAK-STAT signaling pathway. These findings provide novel perspectives and directions for further exploration of the regulatory mechanisms of lncRNAs toward CPB2 toxin-induced diarrhea in piglets.

Data availability statement

The datasets presented in this study can be found in online repositories. The names of the repository/repositories

and accession number(s) can be found below: <https://www.ncbi.nlm.nih.gov/>, PRJNA749943.

Author contributions

SG and JY: conceived and designed the study. JY, JZ, QY, XH, ZY, PW, and XG: experimental investigation and data analysis. JY, JL, NL, and YG: data curation. JY: writing—original draft. QY: writing—review and editing. All authors have read and agreed to the published version of the manuscript.

Funding

This research was funded by the National Natural Science Foundation of China (31960646) and breeding of new resistant local pig breeds (supporting lines) in the Northern Region (2021YFD1301204).

Acknowledgments

We thank LC-Bio Tech Co., Ltd. (Hangzhou, China) for their assistance with sequencing and data processing.

Conflict of interest

NL and YG were employed by Jilin Rongtai Agricultural Development Co., Ltd.

The remaining authors declare that the research was conducted in the absence of any commercial or financial relationships that could be construed as a potential conflict of interest.

Publisher's note

All claims expressed in this article are solely those of the authors and do not necessarily represent those of their affiliated organizations, or those of the publisher, the editors and the reviewers. Any product that may be evaluated in this article, or claim that may be made by its manufacturer, is not guaranteed or endorsed by the publisher.

Supplementary material

The Supplementary Material for this article can be found online at: <https://www.frontiersin.org/articles/10.3389/fmicb.2022.1082025/full#supplementary-material>

References

- Ashok, D., Papanicolaou, K., Liu, T., and O'Rourke, B. (2020). Reverse-mode mitochondrial $\text{Na}^+/\text{Ca}^{2+}$ exchange, not the MCU, is the primary mode of Ca^{2+} import into the mitochondria during ischemia/reperfusion in neonatal cardiac myocytes. *Biophys. J.* 118:407a. doi: 10.1016/j.bpj.2019.11.2305
- Begum, H. M., Mariano, C., Zhou, H., and Shen, K. (2021). E-cadherin regulates mitochondrial membrane potential in cancer cells. *Cancers* 13:5054. doi: 10.3390/cancers13205054
- Bueschel, D. M., Jost, B. H., Billington, S. J., Trinh, H. T., and Songer, J. G. (2003). Prevalence of cpb2, encoding beta2 toxin, in *Clostridium perfringens* field isolates: Correlation of genotype with phenotype. *Vet. Microbiol.* 94, 121–129. doi: 10.1016/S0378-1135(03)00081-6
- Carlevaro-Fita, J., Rahim, A., Guigó, R., Vardy, L. A., and Johnson, R. (2016). Cytoplasmic long noncoding RNAs are frequently bound to and degraded at ribosomes in human cells. *RNA* 22, 867–882. doi: 10.1261/rna.053561.115
- Carrieri, C., Cimatti, L., Biagioli, M., Beugnet, A., Zucchelli, S., Fedele, S., et al. (2012). Long non-coding antisense RNA controls Uchl1 translation through an embedded SINEB2 repeat. *Nature* 491, 454–457. doi: 10.1038/nature11508
- Carrieri, C., Forrest, A. R., Santoro, C., Persichetti, F., Carninci, P., Zucchelli, S., et al. (2015). Expression analysis of the long non-coding RNA antisense to Uchl1 (AS Uchl1) during dopaminergic cells' differentiation in vitro and in neurochemical models of Parkinson's disease. *Front. Cell. Neurosci.* 9:114. doi: 10.3389/fncel.2015.00114
- Chen, J., Zhang, C., Zhang, N., and Liu, G. (2019). Porcine endemic diarrhea virus infection regulates long noncoding RNA expression. *Virology* 527, 89–97. doi: 10.1016/j.virol.2018.11.007
- Deng, D., Tan, X., Han, K., Ren, R., Cao, J., and Yu, M. (2020). Transcriptomic and ChIP-seq integrative analysis reveals important roles of epigenetically regulated lncRNAs in placental development in Meishan pigs. *Genes* 11:397. doi: 10.3390/genes11040397
- Derecka, M., Gornicka, A., Koralov, S. B., Szczepanek, K., Morgan, M., Rajc, V., et al. (2012). Tyk2 and Stat3 regulate brown adipose tissue differentiation and obesity. *Cell Metab.* 16, 814–824. doi: 10.1016/j.cmet.2012.11.005
- Derrien, T., Johnson, R., Bussotti, G., Tanzer, A., Djebali, S., Tilgner, H., et al. (2012). The GENCODE v7 catalog of human long noncoding RNAs: Analysis of their gene structure, evolution, and expression. *Genome Res.* 22, 1775–1789. doi: 10.1101/gr.132159.111
- Fanucchi, S., Fok, E. T., Dalla, E., Shibayama, Y., Börner, K., Chang, E. Y., et al. (2019). Immune genes are primed for robust transcription by proximal long noncoding RNAs located in nuclear compartments. *Nat. Genet.* 51, 138–150. doi: 10.1038/s41588-018-0298-2
- Gao, X., Yang, Q., Huang, X., Yan, Z., and Gun, S. (2020). Effects of *Clostridium perfringens* beta2 toxin on apoptosis, inflammation, and barrier function of intestinal porcine jejunum epithelial cells. *Microb. Pathog.* 147:104379. doi: 10.1016/j.micpath.2020.104379
- Guo, C.-J., Ma, X.-K., Xing, Y.-H., Zheng, C.-C., Xu, Y.-F., Shan, L., et al. (2020). Distinct processing of lncRNAs contributes to non-conserved functions in stem cells. *Cell* 181, 621–636.e22. doi: 10.1016/j.cell.2020.03.006
- Guttman, M., Donaghey, J., Carey, B. W., Garber, M., Grenier, J. K., Munson, G., et al. (2011). lincRNAs act in the circuitry controlling pluripotency and differentiation. *Nature* 477, 295–300. doi: 10.1038/nature10398
- Hartford, C. C. R., and Lal, A. (2020). When long noncoding becomes protein coding. *Mol. Cell. Biol.* 40:e00528-19. doi: 10.1128/MCB.00528-19
- Holzinger, D., Jorns, C., Stertz, S., Boisson-Dupuis, S., Thimme, R., Weidmann, M., et al. (2007). Induction of MxA gene expression by influenza A virus requires type I or type III interferon signaling. *J. Virol.* 81, 7776–7785. doi: 10.1128/JVI.00546-06
- Huang, X. Y., Sun, W. Y., Yan, Z. Q., Shi, H. R., Yang, Q. L., Wang, P. F., et al. (2019). Novel insights reveal anti-microbial gene regulation of piglet intestine immune in response to *Clostridium perfringens* infection. *Sci. Rep.* 9:1963. doi: 10.1038/s41598-018-37898-5
- Jia, Y., Liu, T., Zhou, L., Zhu, J., Wu, J., Sun, D., et al. (2016). Effects of di-(2-ethylhexyl) phthalate on lipid metabolism by the JAK/STAT pathway in rats. *Int. J. Environ. Res. Public Health* 13:1085. doi: 10.3390/ijerph13111085
- Jin, K., Wang, S., Zhang, Y., Xia, M., Mo, Y., Li, X., et al. (2019). Long non-coding RNA PVT1 interacts with MYC and its downstream molecules to synergistically promote tumorigenesis. *Cell. Mol. Life Sci.* 76, 4275–4289. doi: 10.1007/s00018-019-03222-1
- Kanehisa, M., Araki, M., Goto, S., Hattori, M., Hirakawa, M., Itoh, M., et al. (2007). KEGG for linking genomes to life and the environment. *Nucleic Acids Res.* 36(Suppl. 1), D480–D484. doi: 10.1093/nar/gkm882
- Kim, D., Langmead, B., and Salzberg, S. L. (2015). HISAT: A fast spliced aligner with low memory requirements. *Nat. Methods* 12, 357–360. doi: 10.1038/nmeth.3317
- Kong, L., Zhang, Y., Ye, Z.-Q., Liu, X.-Q., Zhao, S.-Q., Wei, L., et al. (2007). CPC: Assess the protein-coding potential of transcripts using sequence features and support vector machine. *Nucleic Acids Res.* 35(Suppl. 2), W345–W349. doi: 10.1093/nar/gkm391
- Kretz, M., Siprashvili, Z., Chu, C., Webster, D. E., Zehnder, A., Qu, K., et al. (2013). Control of somatic tissue differentiation by the long non-coding RNA TINCR. *Nature* 493, 231–235. doi: 10.1038/nature11661
- Lebrun, M., Filée, P., Mousset, B., Desmecht, D., Galleni, M., Mainil, J., et al. (2007). The expression of *Clostridium perfringens* consensus beta2 toxin is associated with bovine enterotoxaemia syndrome. *Vet. Microbiol.* 120, 151–157. doi: 10.1016/j.vetmic.2006.10.020
- Lee, K., Um, S. H., Rhee, D. K., and Pyo, S. (2016). Interferon-alpha inhibits adipogenesis via regulation of JAK/STAT1 signaling. *Biochim. Biophys. Acta Gen. Subj.* 1860, 2416–2427. doi: 10.1016/j.bbagen.2016.07.009
- Ljvak, K. (2001). Analysis of relative gene expression data using real time quantitative PCR and the $2^{-\Delta\Delta\text{CT}}$ method. *Methods* 25, 402–408. doi: 10.1006/meth.2001.1262
- Lu, H., Wu, S., Chen, H., Huang, Y., Qiu, G., Liu, L., et al. (2018). Crizotinib induces apoptosis of lung cancer cells through JAK-STAT pathway. *Oncol. Lett.* 16, 5992–5996. doi: 10.3892/ol.2018.9387
- Luo, R., Yang, Q., Huang, X., Yan, Z., Gao, X., Wang, W., et al. (2020). *Clostridium perfringens* beta2 toxin induced in vitro oxidative damage and its toxic assessment in porcine small intestinal epithelial cell lines. *Gene* 759:144999. doi: 10.1016/j.gene.2020.144999
- Marzia, D., Andrea, P., Filomena, F. P., Giuseppe, P., Elisa, T., Claudio, L., et al. (2018). Long non-coding RNAs play a role in the pathogenesis of psoriatic arthritis by regulating MicroRNAs and genes involved in inflammation and metabolic syndrome. *Front. Immunol.* 9:1533. doi: 10.3389/fimmu.2018.01533
- Mercer, T. R., Neph, S., Dinger, M. E., Crawford, J., Smith, M. A., Shearwood, A.-M. J., et al. (2011). The human mitochondrial transcriptome. *Cell* 146, 645–658. doi: 10.1016/j.cell.2011.06.051
- Muoz-Cánoves, P., Scheele, C., Pedersen, B. K., and Serrano, A. L. (2013). Interleukin-6 myokine signaling in skeletal muscle: A double-edged sword? *FEBS Lett.* 280, 4131–4148. doi: 10.1111/FEBS.12338
- Noh, J. H., Kim, K. M., Abdelmohsen, K., Yoon, J. H., Panda, A. C., Munk, R., et al. (2016). HuR and GRSF1 modulate the nuclear export and mitochondrial localization of the lncRNA RMRP. *Genes Dev.* 20, 1224–1239. doi: 10.1101/gad.276022.115
- O'Donnell, M. A., Perez-Jimenez, E., Oberst, A., Ng, A., Massoumi, R., Xavier, R., et al. (2011). Caspase 8 inhibits programmed necrosis by processing CYLD. *Nat. Cell Biol.* 13, 1437–1442. doi: 10.1038/ncb2362
- O'Shea, J. J., Schwartz, D. M., Villarino, A. V., Gadina, M., McInnes, I. B., and Laurence, A. (2015). The JAK-STAT pathway: Impact on human disease and therapeutic intervention. *Annu. Rev. Med.* 66, 311–328. doi: 10.1146/annurev-med-051113-024537
- Pavlovic, J., Haller, O., and Staeheli, P. (1992). Human and mouse Mx proteins inhibit different steps of the influenza virus multiplication cycle. *J. Virol.* 66, 2564–2569. doi: 10.1016/0166-0934(92)90025-9
- Raftery, N., and Stevenson, N. J. (2017). Advances in anti-viral immune defence: Revealing the importance of the IFN JAK/STAT pathway. *Cell. Mol. Life Sci.* 74, 2525–2535. doi: 10.1007/s00018-017-2520-2
- Richard, A., and Stephens, J. M. (2014). The role of JAK-STAT signaling in adipose tissue function. *Biochim. Biophys. Acta* 1842, 431–439. doi: 10.1016/j.bbadis.2013.05.030
- Si, L., Yang, X., Yan, X., Wang, Y., and Zheng, Q. (2017). Isoliquiritigenin induces apoptosis of human bladder cancer T24 cells via a cyclin-dependent kinase-independent mechanism. *Corrigendum in. Oncol. Lett.* 14, 241–249. doi: 10.3892/ol.2021.12529
- Silva, R., Junior, C. O., Guedes, R., and Lobato, F. (2015). *Clostridium perfringens*: A review of the disease in pigs, horses and broiler chickens. *Cienc. Rural* 45, 1027–1034. doi: 10.1590/0103-8478cr20140927

- Spitaels, J., Hoecke, L. V., Roose, K., Kochs, G., and Saelens, X. (2019). Mx1 in hematopoietic cells protects against thogoto virus infection. *J. Virol.* 93:e00193-19. doi: 10.1128/JVI.00193-19
- Stattello, L., Guo, C.-J., Chen, L. L., and Huarte, M. (2020). Gene regulation by long non-coding RNAs and its biological functions. *Nat. Rev. Mol. Cell Biol.* 22, 96–118. doi: 10.1038/s41580-020-00315-9
- Sun, L., Luo, H., Bu, D., Zhao, G., Yu, K., Zhang, C., et al. (2013). Utilizing sequence intrinsic composition to classify protein-coding and long non-coding transcripts. *Nucleic Acids Res.* 41:e166. doi: 10.1093/nar/gkt646
- Sun, Z.-Y., Jian, Y.-K., Zhu, H.-Y., and Li, B. (2019). lncRNAPVT1 targets miR-152 to enhance chemoresistance of osteosarcoma to gemcitabine through activating c-MET/PI3K/AKT pathway. *Pathol. Res. Pract.* 215, 555–563. doi: 10.1016/j.prp.2018.12.013
- Tan, J., Xiang, L., and Xu, G. (2019). lncRNA MEG3 suppresses migration and promotes apoptosis by sponging miR-548d-3p to modulate JAK-STAT pathway in oral squamous cell carcinoma. *IUBMB Life* 71, 882–890. doi: 10.1002/iub.2012
- Tian, B., and Manley, J. L. (2017). Alternative polyadenylation of mRNA precursors. *Nat. Rev. Mol. Cell Biol.* 18, 18–30. doi: 10.1038/nrm.2016.116
- Tian, M., Sun, J., Dong, B., and Lin, W. (2019). Construction of mitochondria-nucleolus shuttling fluorescent probe for the reversible detection of mitochondrial membrane potential. *Sens. Actuators B Chem.* 292, 16–23. doi: 10.1016/j.snb.2019.04.118
- Timoney, J., Hartmann, M., Fallon, L., Fallon, E., and Walker, J. (2005). Antibody responses of mares to prepartum vaccination with *Clostridium perfringens* bacterin and beta 2 toxin. *Vet. Rec.* 157, 810–812. doi: 10.1136/vr.157.25.810
- Trapnell, C., Williams, B. A., Pertea, G., Mortazavi, A., Kwan, G., Van Baren, M. J., et al. (2010). Transcript assembly and quantification by RNA-Seq reveals unannotated transcripts and isoform switching during cell differentiation. *Nat. Biotechnol.* 28, 511–515. doi: 10.1038/nbt.1621
- Tumpey, T. M., Szretter, K. J., Van Hoven, N., Katz, J. M., Kochs, G., Haller, O., et al. (2007). The Mx1 gene protects mice against the pandemic 1918 and highly lethal human H5N1 influenza viruses. *J. Virol.* 81, 10818–10821. doi: 10.1128/JVI.01116-07
- Waters, M., Savoie, A., Garmory, H. S., Bueschel, D., Popoff, M. R., Songer, J. G., et al. (2003). Genotyping and phenotyping of beta2-toxigenic *Clostridium perfringens* fecal isolates associated with gastrointestinal diseases in piglets. *J. Clin. Microbiol.* 41, 3584–3591. doi: 10.1128/JCM.41.8.3584-3591.2003
- Wenzel, A., Akbasli, E., and Gorodkin, J. (2012). RSearch: Fast RNA-RNA interaction search using a simplified nearest-neighbor energy model. *Bioinformatics* 28, 2738–2746. doi: 10.1093/bioinformatics/bts519
- Willson, J. (2019). A matter of life and death for caspase 8. *Nat. Rev. Mol. Cell Biol.* 21:63. doi: 10.1038/s41580-019-0201-8
- Wu, Z., Fan, H., Jin, J., Gao, S., Huang, R., Wu, S., et al. (2022). Insight into mechanisms of pig lncRNA FUT3-AS1 regulating *E. coli* F18-bacterial diarrhea. *PLoS Pathog.* 18:e1010584. doi: 10.1371/journal.ppat.1010584
- Yang, J., Zhang, J., Gao, X., Luo, R., Xie, K., Wang, W., et al. (2022). FTO regulates apoptosis in CPB2-treated IPEC-J2 cells by targeting caspase 3 apoptotic protein. *Animals* 12:1644. doi: 10.3390/ani12131644
- Yao, Q., Li, Z., and Chen, D. (2022). Review of LINC00707: A novel lncRNA and promising biomarker for human diseases. *Front. Cell Dev. Biol.* 10:813963. doi: 10.3389/fcell.2022.813963
- Young, M. D., Wakefield, M. J., Smyth, G. K., and Oshlack, A. (2010). Gene ontology analysis for RNA-seq: Accounting for selection bias. *Genome Biol.* 11:R14. doi: 10.1186/gb-2010-11-2-r14
- Zeng, J., Song, F., Yang, Y., Ma, C., Deng, G., Li, Y., et al. (2016). The generation and characterization of recombinant protein and antibodies of *Clostridium perfringens* beta2 toxin. *J. Immunol. Res.* 2016:5708468. doi: 10.1155/2016/5708468
- Zhao, J., Du, P., Cui, P., Qin, Y., Hu, C. E., Wu, J., et al. (2018). lncRNA PVT1 promotes angiogenesis via activating the STAT3/VEGFA axis in gastric cancer. *Oncogene* 37, 4094–4109. doi: 10.1038/s41388-018-0250-z
- Zhao, L., Xia, M., Wang, K., Lai, C., Fan, H., Gu, H., et al. (2020). A long non-coding RNA IVRPIE promotes host antiviral immune responses through regulating interferon β 1 and ISG expression. *Front. Microbiol.* 20:260. doi: 10.3389/fmicb.2020.00260
- Zhao, X., Cheng, Z., and Wang, J. (2018). Long noncoding RNA FEZF1-AS1 promotes proliferation and inhibits apoptosis in ovarian cancer by activation of JAK-STAT3 pathway. *Med. Sci. Monit.* 12, 8088–8095. doi: 10.12659/MSM.911194
- Zhaojun, C., Lulin, T., Xin, F., Abdel-Nasser, S., Zunguo, L., and Xiong, L. (2022). Hydroxy- γ -sanshool from *Zanthoxylum bungeanum* (prickly ash) induces apoptosis of human colorectal cancer cell by activating P53 and Caspase 8. *Front. Nutr.* 1:914638. doi: 10.3389/fnut.2022.914638